ACS APPLIED MATERIALS & INTERFACES

Research Article

www.acsami.org

Controlled Architecture of Dual-Functional Block Copolymer Brushes on Thin-Film Composite Membranes for Integrated "Defending" and "Attacking" Strategies against Biofouling

Gang Ye,*[,†] Jongho Lee,[‡] François Perreault,[‡] and Menachem Elimelech*[,‡]

[†]Institute of Nuclear and New Energy Technology, Collaborative Innovation Center of Advanced Nuclear Energy Technology, Beijing Key Lab of Radioactive Waste Treatment, Tsinghua University, Beijing 100084, China

[‡]Department of Chemical and Environmental Engineering, Yale University, New Haven, Connecticut 06520, United States

Supporting Information

ABSTRACT: We report a new macromolecular architecture of dual functional block copolymer brushes on commercial thin-film composite (TFC) membranes for integrated "defending" and "attacking" strategies against biofouling. Mussel-inspired catechol chemistry is used for a convenient immobilization of initiator molecules to the membrane surface with the aid of polydopamine (PDA). Zwitterionic polymer brushes with strong hydration capacity and quaternary ammonium salt (QAS) polymer brushes with bactericidal ability are sequentially grafted on TFC membranes via activators regenerated by electron transfer–atom transfer radical polymerization (ARGET-ATRP), an environmentally benign and controlled polymerization method. Measurement of membrane intrinsic transport properties in reverse osmosis experiments shows that the modified TFC membrane maintains the same water permeability and salt selectivity as the pristine TFC membrane. Chemical force microscopy and protein/bacterial adhesion studies are carried out for a comprehensive evaluation of the biofouling resistance and antimicrobial ability, demonstrating low biofouling propensity and excellent bacterial inactivation for the modified TFC membrane. We conclude that this polymer architecture, with complementary "defending" and "attacking" capabilities, can effectively prevent the attachment of biofoulants and formation of biofilms and thereby significantly mitigate biofouling on TFC membranes.

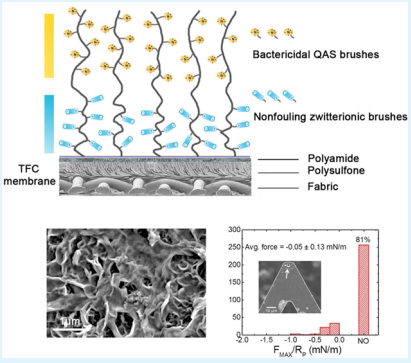

KEYWORDS: *thin-film composite (TFC) membranes, antifouling, antimicrobial, ARGET-ATRP, block copolymers*

1. INTRODUCTION

Thin-film composite (TFC) polyamide membranes play a critical role in state-of-the-art reverse osmosis (RO), a rapidly growing desalination technology for global water production.[1,2] However, a major drawback of using TFC membranes is their high propensity toward biofouling. Biofouling is initiated by the attachment of biomacromolecules or microorganisms and the subsequent formation of a biofilm, which significantly impairs membrane performance by decreasing membrane water permeability, selectivity, and life span.[3−5] Consequently, during the past decade, extensive research efforts have been devoted to developing TFC membranes with superior biofouling-resistant properties.[6,7]

Antibiofouling strategies using surface modification can be classified into two mechanisms: resistance to adhesion of biocontaminants ("defending") and degradation of the biocontaminants ("attacking").[8] It is generally accepted that a hydrophilic surface offers biofouling resistance because of the hydrophobic nature of biofoulants such as proteins.[9−11] A classic "defending" protocol, therefore, involves modification of membrane surface chemistry to increase hydrophilicity by introducing poly(ethylene glycol) (PEG) or oligo(ethylene glycol).[12−14] However, studies have shown that PEG naturally degrades by oxidation, especially in complex media, and is not suitable for long-term use.[15,16]

Alternatively, zwitterionic polymers with a balanced charge and minimized net dipole have proven to be excellent candidates as nonfouling materials due to their strong hydration capacity via electrostatic interactions.[17−24] Surface functionalization with zwitterionic amino acids,[25] polymers,[26,27] biopolymers,[28] and copolymers[29,30] has been shown to improve the fouling resistance of polyamide TFC membranes toward proteins, humic acid, alginate, and bacteria. Unlike their PEG counterparts, zwitterionic polymers have better stability, broader chemical diversity, and greater freedom for molecular design, thus representing an excellent antifouling agent for membrane functionalization.

The "attacking" strategy, on the other hand, involves membrane functionalization with releasable bacteria-killing substances, such as silver nanoparticles (Ag NPs)[31] and antibiotics,[32] or decoration with bactericidal functionalities like quaternary ammonium salts (QAS),[33−35] graphene oxide,[36]

Received: July 22, 2015
Accepted: September 17, 2015
Published: September 17, 2015

DOI: 10.1021/acsami.5b06647
ACS Appl. Mater. Interfaces 2015, 7, 23069−23079

and photoactive agents[37] for contact killing. Inactivation of bacterial cells on the surface was found to reduce the rate of biofilm formation on biocide-functionalized membranes,[38−40] demonstrating the potential of antimicrobial membrane design for biofouling prevention.

However, all approaches mentioned above have fundamental limitations for long-term biofouling resistance in complex biological environments. Protein-resisting PEG surfaces have been proven to be ineffective in preventing bacterial deposition and colonization,[16,41] and bactericidal surfaces suffer from the rapid accumulation of dead bacterial cells, which shield the surface functional groups and provide an accessible platform for microorganisms to attach and proliferate.[42−44] For this reason, numerous researchers in recent years have attempted to combine these two complementary biofouling mitigation strategies to impart both nonadhesive and bactericidal capabilities on the membrane surfaces.

Tiller et al. developed a Ag NP-embedded surface that was additionally modified with a bacteria-repelling PEG polymer network. The surface was demonstrated to be capable of inhibiting bacterial growth and repelling microbes at the same time.[45] Lienkamp and co-workers also reported a bifunctional surface by integrating the nonfouling property of poly(zwitterion) with the bactericidal ability of synthetic antimicrobial peptides (AMPs).[46] Most recently, a "kill-and-release" strategy was proposed to build an antimicrobial surface based on a cationic ester. The cationic ester-functionalized surface was able to kill the attached bacteria and release dead microbes upon the hydrolysis of ester groups, resulting in a nonfouling zwitterionic surface.[47]

Overall, these novel strategies and materials are encouraging, but they still suffer from short-term efficiency, limited stability in complex environments, and impairment of membrane permeability or selectivity. Additional efforts are therefore required to seek out more reliable and efficient antibiofouling approaches without compromising membrane performance.

Here, we present a new environmentally benign and robust approach to integrate both "defending" and "attacking" antibiofouling strategies in TFC membranes via the controllable architecture of a dual-functional diblock copolymer by using an improved atom-transfer radical-polymerization (ATRP) technique. Surface-initiated ATRP has been widely recognized as a powerful technique for antifouling surface construction. It provides a unique route to dense polymer brushes with narrow polydispersity, controlled architecture, and well-defined thickness and composition.[48−52] As a milestone of the development of ATRP techniques, activators regenerated by electron transfer−atom transfer radical polymerization (ARGET-ATRP) require a smaller amount of copper catalyst and tolerate a limited amount of oxygen.[53−56] This development paved the way for convenient use of ATRP to modify large membrane surface areas under ordinary laboratory and industrial conditions.

In this study, we show that nonfouling zwitterionic polymer brushes and antimicrobial QAS polymer brushes can be sequentially grown by ARGET-ATRP onto the surface of TFC membranes. To our knowledge, this is the first case of controlled architecture of dual-functional block-type polymers on TFC membranes via surface-initiated ATRP techniques. The polymerization is initiated by 2-bromoisobutyryl bromide (BiBB), which is covalently bonded to mussel-inspired polydopamine (PDA) for immobilization onto the membrane surface.[57] Results show that the diblock copolymer grafted TFC RO membranes have excellent resistance against the nonspecific adsorption of proteins due to the function of the zwitterionic layer. Furthermore, the QAS brushes effectively kill adsorbed bacteria, which are then easily released from the membrane because of the presence of zwitterionic brushes. Notably, this macromolecular architecture protocol via ARGET-ATRP provides good stability and does not impact intrinsic membrane transport properties.

2. EXPERIMENTAL SECTION

2.1. Chemicals. [2-(Methacryloyloxy)ethyl]trimethylammonium chloride solution (MTAC) (80 wt % in H_2O), [2-(methacryloyloxy)-ethyl]dimethyl-(3-sulfopropyl)ammonium hydroxide (also named "sulfobetaine methacrylate", SBMA), α-bromoisobutyryl bromide (BiBB) (98%), dopamine hydrochloride, triethylamine (TEA) (>99%), tris(hydroxymethyl)aminomethane (Tris) (>99.8%), copper(II) chloride, tris(2-pyridylmethyl)amine (TPMA), L-ascorbic acid, and *N,N*-dimethylformamide (DMF) were purchased from Sigma-Aldrich. Commercial TFC membranes were provided by Dow Chemical (SW30 XLE). Deionized (DI) water was obtained from a Milli-Q ultrapure water purification system (Millipore, Billerica, MA). The LIVE/DEAD Baclight bacterial viability kit, containing propidium iodide (PI) and Syto 9, was obtained from Thermo Fisher Scientific (Molecular Probes, Grand Island, NY).

2.2. Preparation of Poly(SBMA-*b*-MTAC)-Grafted TFC Membrane. Commercial RO membranes were immersed in 25% isopropanol for 30 min. Then, the membranes were washed with distilled water and soaked in Milli-Q water overnight. Dopamine hydrochloride (800 mg, 4.20 mmol) was dissolved in 40 mL DMF in an amber bottle with a PTFE/silicone septum. After the solution was degassed, 2-bromoisobutyryl bromide (0.26 mL, 2.10 mmol) and triethylamine (0.30 mL, 2.10 mmol) were added. The reaction lasted for 3 h under stirring at room temperature.

A wetted membrane was sandwiched between a clean glass plate and a rubber mat with a central hole cut out (i.e., hole: 25 cm long, 15 cm width) on a rocking platform. The sandwich was secured by steel clamps, thus creating a sealed well. The dopamine-BiBB in DMF was added to aqueous tris(hydroxymethyl)aminomethane buffer at pH 8.5 (900 mg, 4.0×10^{-3} mol in 200 mL Milli-Q water), and the solution was then immediately added to the well. The entire solution was constantly moved over the membrane surface using the rocking platform at ambient conditions. After 10 min, the PDA-BiBB-deposited membrane was removed from the glass plate and thoroughly rinsed with distilled water. The washed membranes were stored in aqueous isopropanol (10% v/v) until further modification.

Sulfobetaine methacrylate (SBMA) (7.82 g, ~28 mmol) was dissolved in a 1:1 isopropanol:Milli-Q water mixture (100 mL, v/v) in a bottle (covered with aluminum foil) with a septa lid. After degassing by bubbling through dry N_2 for 10 min, a solution of copper(II) chloride (0.002 g, ~14.8 μmol) and TPMA (0.028 g, ~0.095 mmol) in 1:1 isopropanol:Milli-Q water (4 mL, v/v) was then syringed into the bottle.

The PDA-BiBB deposited membrane was placed into a 250 mL bottle (covered with aluminum foil). The zwitterionic monomer solution (100 mL) prepared above was introduced into the bottle. The systems were degassed by N_2 for 10 min. A solution of ascorbic acid in 1:1 isopropanol:water (0.4 g, ~2.2 mmol, in 4 mL v/v) was then syringed into the bottles. This initiated the polymerization, which was undertaken for 1 h. Then, the bottle was opened to air to terminate the reaction. The poly(sulfobetaine methacrylate) (PSBMA)-grafted membrane was washed thoroughly with Milli-Q water to remove the unreacted monomers.

[2-(Methacryloyloxy)ethyl]trimethylammonium chloride solution (MTAC) (7.26 g, ~28 mmol MTAC) was dissolved in a 1:1 isopropanol:Milli-Q water mixture (100 mL, v/v) in a bottle (covered with aluminum foil) with a septa lid. After degassing by bubbling through dry N_2 for 10 min, a solution of copper(II) chloride (0.002 g, ~14.8 μmol) and tris(2-pyridylmethyl)amine (TPMA) (0.028 g, ~96.4 μmol) in 1:1 isopropanol:Milli-Q water (4 mL, v/v) was

DOI: 10.1021/acsami.5b06647
ACS Appl. Mater. Interfaces 2015, 7, 23069−23079

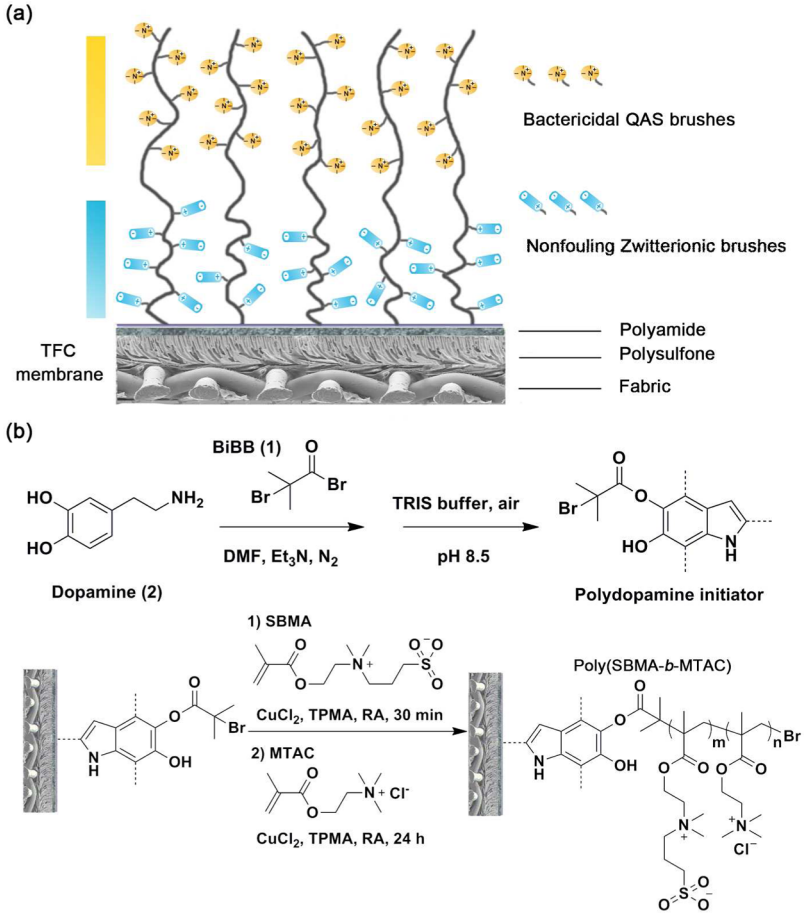

Figure 1. Illustration of the structure of dual-functional block polymer brushes on a TFC membrane for integrated antifouling strategy (a) and surface-initiated ARGET-ATRP synthesis of the poly(SBMA-*b*-MTAC) from the TFC membrane (b). The initiator BiBB (1) is coupled with dopamine (2) for immobilization onto the surface of the TFC membrane in pH 8.5 Tris buffer.

syringed into the bottle. Then, the solution was added to a 250 mL bottle containing the PSBMA-grafted membrane. The system was degassed by a N_2 purge for 10 min. A solution of ascorbic acid in 1:1 isopropanol:water (0.4 g, ~2.2 mmol, in 4 mL v/v) was syringed into the bottle. The polymerization was undertaken for 24 h. The poly(sulfobetaine methacrylate)-*block*-poly([2-(methacryloyloxy)-ethyl]trimethylammonium chloride) (abbreviated as "poly(SBMA-*b*-MTAC)")-modified membrane was washed with Milli-Q water and stored in aqueous isopropanol (10% v/v).

2.3. BSA Adsorption Test. Fluorescein-conjugated BSA (FITC-BSA) was purchased from Life Technologies (A23015, 5 mg), and 1 mL of phosphate-buffer saline (PBS) at pH 7.4 was added to dissolve completely. The solution was centrifuged for ~10 s at 12,000 rpm. The supernatants were then taken and diluted with PBS to a concentration of 0.05 mg/mL. For each pristine and modified membrane, two pieces with a diameter of 2.1 cm were cut and mounted in a homemade membrane cell on a rocking plate (60 rpm) with the active layer (salt rejecting) side in contact with the prepared FITC-BSA solution for 3 h in the dark. After the solution was removed from the cell, the membrane pieces were rinsed twice by gently adding 2 mL of PBS and removed from the cell after 1 min on the rocking platform at the same speed. The rinsed membrane piece was placed on a glass slide with a droplet of PBS on it, covered by a cover glass. The cover glass was sealed by nail polish to prevent any evaporation of the PBS during fluorescence imaging. The prepared sample was then mounted on an inverted Axiovert 200 M epifluorescence microscope (Carl Zeiss Inc., Thornwood, NY, USA). For each sample, at least ten spots were randomly selected, and fluorescence images were acquired.

2.4. AFM Adhesion Force Measurement. A particle-functionalized AFM cantilever was used to quantify the adhesion forces between the membrane and a carboxylated latex particle, which serves as a general model for organic foulants.[58] Tipless SiN cantilevers (Bruker NP-O10) were cleaned before functionalization in a UV/ozone cleaner for 20 min (BioForce Nanosciences, Ames, IA). Then, a carboxyl-modified latex particle having a diameter of 4 μm (CML, carboxyl content 19.5 μeq/g, Life Technologies, Eugene, OR) was glued to the tip of the cantilever using UV-curable adhesive (Norland Optical Adhesive 68, Norland Products, Cranbury, NJ) and cured for 20 min in the UV/ozone cleaner.

Force measurements were collected with a Dimension Icon AFM (Bruker, Santa Barbara, CA). Solution chemistry used for the adhesion force measurement was 50 mM NaCl and 5 mM $CaCl_2$.[59] Force curves were collected using a trigger force of 10 nN, a ramp size of 1 μm, and a ramp rate of 0.5 Hz. The cantilever deflection sensitivity and spring constant were determined before each experiment using the thermal noise method.[60] Adhesion forces were determined using the Peak Analysis function of Nanoscope Analysis v1.5 (Bruker), using data converted from cantilever deflection relative to piezoelectric stage retraction to force relative to particle−membrane separation.

2.5. Antimicrobial Test. *Escherichia coli* (ATCC BW26437, Yale Coli Genetic Stock Center, New Haven, CT) cells were transferred from a solid agar culture to Lysogeny broth (LB) broth and grown at 37 °C overnight. The bacterial cultures were brought to log phase by diluting the overnight culture (1:25) with fresh LB medium and growing them until they reached an optical density at 600 nm (OD600 nm) of 1.0, which is equal to ~10^9 colony forming units (CFU) per mL. The cultures were then washed three times with fresh sterile PBS and resuspended in PBS at a final concentration of ~10^9 CFU/mL.

To evaluate the antimicrobial activity of the different modified membranes, we punched coupons of ~3.5 cm^2 from each membrane

DOI: 10.1021/acsami.5b06647
ACS Appl. Mater. Interfaces 2015, 7, 23069−23079

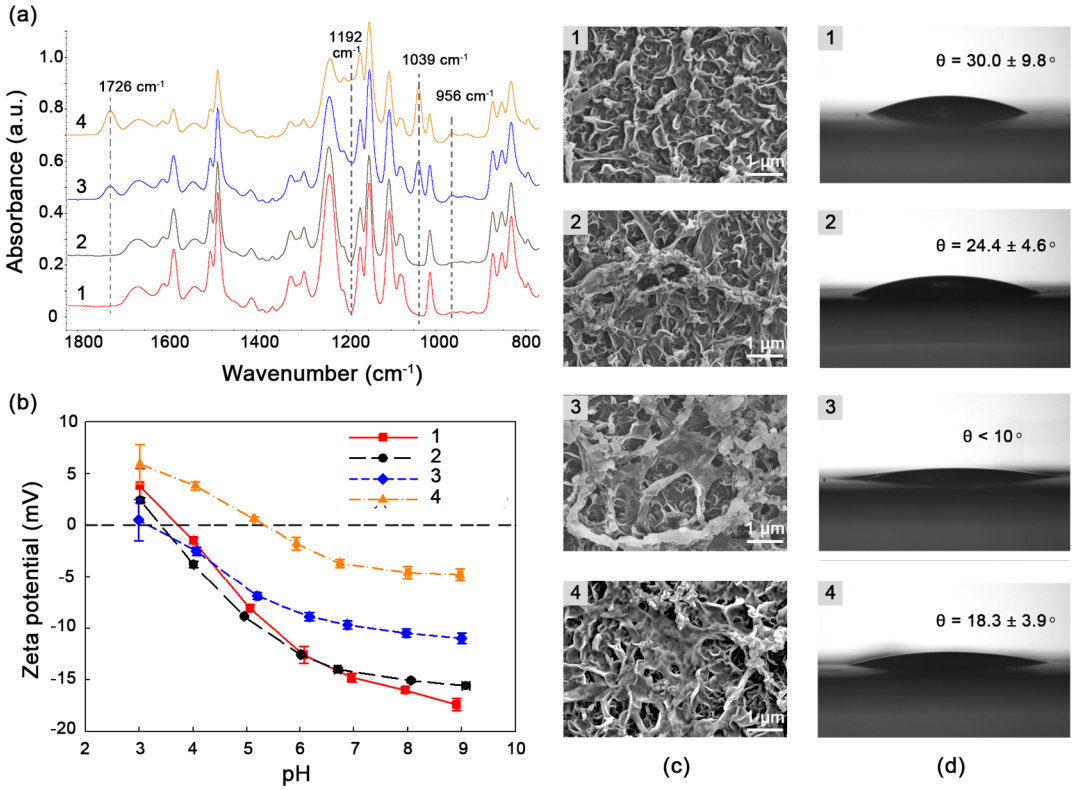

Figure 2. ATR FTIR spectra (a), zeta potential (b), SEM surface morphology (c), and water contact angle measurements (d) of TFC membranes in the modification process. (1) Pristine TFC membrane, (2) PDA-BiBB immobilized membrane, (3) PSBMA-grafted membrane, and (4) poly(SBMA-*b*-MTAC)-grafted membrane.

and placed them in plastic holders to expose only the active layer to bacteria. Bacterial suspensions (3 mL) were contacted with the membrane for 3 h at room temperature. The bacterial suspension was then discarded, and the membranes were washed twice with fresh PBS, as described in section 2.3, to remove nonattached cells. Cell viability of the attached cells was determined by the LIVE/DEAD fluorescent staining assay (LIVE/DEAD *Bac*Light viability assay, Molecular Probes, NY). Cells deposited on the membranes were stained with 3.34 μM Syto 9 and 20 μM propidium iodide in PBS for 30 min. The staining solution was removed, and the membranes were rinsed once with PBS before being mounted on a microscopic slide for epifluorescence microscopy. Ten pictures per replicate were taken with an Axiovert 200 M epifluorescence microscope (Carl Zeiss Inc., Thornwood, NY, USA). Live (green) and dead (red) cells were counted with the ImageJ Cell Counter Plugin (National Institutes of Health, MD).

3. RESULTS AND DISCUSSION

3.1. Block Copolymer Architecture on TFC Membranes. *3.1.1. Synthesis Strategy.* Because of the low usage of catalyst and tolerance to oxygen, ARGET-ATRP holds great promise for surface modification of large-area membranes under industry friendly conditions.[53−56] In this study, by using a surface-initiated ARGET-ATRP technique, macromolecular engineering on TFC membranes was implemented for building block-type polymer brushes, which aimed to impart TFC membranes with combined nonadhesive and antimicrobial properties. The architecture of dual-functional block copolymers on TFC membranes for an integrated antifouling strategy is illustrated in Figure 1. Zwitterionic poly(sulfobetaine methacrylate) (PSBMA) brushes and poly[2-(methacryloyloxy)ethyl]trimethylammonium chloride (PMTAC) brushes, a QAS polymer, were sequentially grown from the surface of the TFC membrane. The zwitterionic PSBMA brushes are responsible for preventing the nonspecific attachment/adsorption of biofoulants, and the QAS PMTAC brushes provide antimicrobial activity. Moreover, the zwitterionic brushes with strong hydration ability generate a favorable environment for the release of the dead microbes killed by the QAS brushes, thus preventing the formation of biofilms that can shield the surface functional groups on TFC membranes.[42]

As illustrated in Figure 1, the initiator BiBB (**1**) was first coupled with dopamine (**2**), followed by immobilization onto the surface of the TFC membrane using mussel-inspired catechol chemistry.[61−63] At present, the mechanism of PDA assembly in an alkaline environment is not well understood. It has been suggested that the oxidation of catechol groups of dopamine to quinone is the critical control point in the polymerization.[64] Next, initiated by the PDA-immobilized BiBB, zwitterionic PSBMA brushes were grown from the surface of the TFC membrane. To control the thickness of the zwitterionic polymer brushes, we investigated the ARGET-ATRP mediated growth of SBMA on a silicon wafer. The thickness of the PSBMA brushes at different durations of polymerization was examined with a KLA Tencor Alphastep profilometer and by scanning electron microscopy (SEM) (Figure S1). The PSBMA chain showed a rapid propagation rate in the ARGET-ATRP reaction. A 200 nm layer of PSBMA brushes was obtained after a reaction time of 1 h, which we adopted for the growth of PSBMA on the TFC membranes.

The controlled "living" characteristics of ARGET-ATRP enable reinitiation of polymerization after chain termination of one type of polymer, making it possible to obtain block-type polymer brushes for building a multifunctional platform.[65,66] A

DOI: 10.1021/acsami.5b06647
ACS Appl. Mater. Interfaces 2015, 7, 23069−23079

second-stage polymerization was performed to grow PMTAC brushes from the end of the PSBMA chains with bromine initiators. Prior to that, ARGET-ATRP of only an MTAC monomer on the TFC membrane revealed a slow propagation rate of the polymer chain under the same conditions (Figure S2). Therefore, the second-stage polymerization was carried out for 24 h to obtain PMTAC brushes of an adequate chain length, grafted from the end of the PSBMA chains.

3.1.2. Structure Characterization. The structures of the pristine TFC membrane and the ARGET-ATRP-modified membranes were characterized by attentuated total reflectance Fourier transform infrared (ATR FTIR) spectroscopy. Figure 2a shows the 1800−800 cm^{-1} wavenumber region of the FTIR spectra, covering the characteristic absorbances of the main functional groups in the modified membranes. Because the depth of penetration of FTIR (1−5 μm) is larger than a typical polyamide active layer thickness (200−500 nm), combined signals of the polyamide and polysulfone from the support layer are found in the ATR FTIR spectrum of TFC membranes. Absorbances at 1666 and 1539 cm^{-1} correspond to N−C═O and C−N−H vibrations in the amide groups, identified as amide I and amide II modes in secondary amides. The small but clear peak at 1608 cm^{-1} is associated with the hydrogen-bonded carbonyl of the amide. The peaks at 1587, 1504, and 1488 cm^{-1} correspond to skeletal vibration of benzene rings in both polysulfone and polyamide. The peaks associated with the asymmetric stretching and symmetric stretching of the C−SO_2−C groups in polysulfone can be seen at 1323 and 1151 cm^{-1}, respectively. The S═O stretching shows absorbance at 1294 cm^{-1}. The strong peak centered at 1243 cm^{-1} is attributed to the symmetric stretching of C−O−C groups in polysulfone. No evident differences are observed in the ATR FTIR spectra of a pristine TFC membrane and a PDA-BiBB immobilized membrane because a short polymerization time (10 min) in Tris buffer can only introduce a small amount of the PDA-BiBB (as evidenced by an SEM image in the following section). In addition, the absorbances indicative of the functional groups in PDA-BiBB are masked as they overlap with the strong signals of similar functional groups in the polyamide and polysulfone. We note, however, that the area where PDA-BiBB is deposited can be observed by naked eye as a slightly brown coloration on the membrane, which verifies the existence of PDA-BiBB on the TFC membrane.

After the grafting of the PSBMA brushes, new peaks at 1726 and 1039 cm^{-1} were observed in the ATR FTIR spectrum. The former corresponds to the carbonyl in the ester group, and the latter is derived from the symmetric stretch of the sulfonate group in the SBMA molecule. A small but distinct peak appears at 956 cm^{-1}, which is ascribed to the quaternary amine headgroups.[67] This observation suggests that the PSBMA brushes have been successfully grafted onto the PDA-BiBB immobilized TFC membrane. Evidence for successful grafting is also provided by the energy dispersive spectroscopy (EDS) analysis of PSBMA grafted to the surface of the silicon wafer under the same reaction conditions. A clear signal of sulfur atoms in SBMA molecules is identified in Figure S3. The ATR FTIR spectrum of poly(SBMA-*b*-MTAC)-grafted membrane shows similar characteristic peaks as that of the PSBMA-grafted membrane but with intensified absorbance at 1726 and 1192 cm^{-1}, which is associated with the increase in ester groups in the PMTAC brushes.

The surface properties of the modified membranes were further investigated by acquiring zeta potential calculated from streaming potential measurements using the Helmholtz−Smoluchowski equation.[68] The membrane surface streaming potential was measured using an electrokinetic analyzer (EKA, Anton Paar, Germany) with a background electrolyte of 1 mM KCl and 0.1 mM $KHCO_3$ in a channel consisting of two identical membrane surfaces on the top and bottom planes of the channel. As shown in Figure 2b, the zeta potential is indicative of the unique surface characteristics at each membrane modification step. Because of the interfacial polymerization process of typical polyamide TFC membrane fabrication, both unreacted amine and carboxylic groups are available on the pristine TFC membrane surface.[69] The pristine membrane surface charge changes from positive to negative due to deprotonation of the functional groups as pH increases above the isoelectric point of pH 3.7. As the pH increases, the membrane becomes more negatively charged due to deprotonation of the carboxyl group and adsorption of anions, such as Cl^- or OH^-, which are less hydrated than cations, leading to a closer proximity to the surface.[70,71]

The zeta potential was not noticeably altered by PDA-BiBB modification, likely due to the very small thickness and incomplete coverage of the PDA-BiBB layer (as evidenced by SEM images in the following section). However, after the zwitterionic PSBMA brushes were grafted, the magnitude of the zeta potential was markedly reduced, both in positive and negative potential values. The presence of the net zero charge zwitterionic polymers not only covers the underlying charged surface to some extent, but its high affinity to water also leads to swelling of the polymers and physically increases the distance between the electrolyte and the charged surface, which reduces attraction of anions to the surface.[72]

As expected, further modification of the membranes with quaternary ammonium polymers, i.e., poly(SBMA-*b*-MTAC), reduced the negative zeta potential (i.e., more positive charge) with the isoelectric point shifting from pH 3.2 for PSBMA to pH 5.3 for poly(SBMA-*b*-MTAC). Although quaternary ammonium should reveal a positive charge independent of the pH investigated in this study, the zeta potential of the membrane becomes negative at relatively high pH (>5.3); this observation is probably due to incomplete coverage allowing for adsorption of the anions on the uncovered surface, as well as on the quaternary ammonium itself, especially at high pH.[73] These sequential changes in zeta potential clearly indicate successful modification of the pristine TFC membrane with zwitterionic polymers followed by quaternary ammonium polymers.

3.1.3. Surface Morphology and Hydrophilicity. Evidence for the growth of each polymer brush on the membrane was also obtained from morphological changes of the membrane surface (Figure 2c) as well as contact angle measurements at each modification step (Figure 2d). The surface roughness, as measured by atomic force microscopy (AFM), slightly increased after PDA-BiBB modification, probably due to aggregation of PDA (Figure 2c, Figure S4). Further modification with PSBMA and poly(SBMA-*b*-MTAC) gradually smoothed the surface roughness by increasing the thickness of the polymeric coating (Figure S4). However, although a general trend of membrane smoothing by the addition of polymers can be observed, these differences were not statistically significant (Figure S4).

Although PDA should increase hydrophilicity,[74] the change in contact angle on the PDA-BiBB membrane was not prominent, owing to the short reaction time (10 min), resulting

DOI: 10.1021/acsami.5b06647
ACS Appl. Mater. Interfaces 2015, 7, 23069−23079

in incomplete coverage and aggregate formation. After growth of the zwitterionic polymers (PSBMA) was terminated, the surface became superhydrophilic due to the high affinity of the zwitterionic polymer to water.[17] Although the morphology of the poly(SBMA-*b*-MTAC)-deposited membrane was not significantly different from the one with the zwitterionic polymer film, the contact angle increased slightly, indicating reduced coverage of PSBMA blocks by the presence of PMTAC blocks. When PMTAC was polymerized directly after PDA-BiBB, a thin-film structure covering the membrane surface was also observed (Figure S2).

3.2. Water Permeability and Salt Rejection. High water permeability and salt rejection are critically important for reverse osmosis desalination membranes. These membrane performance properties are defined as the water flux across the membrane per a given applied pressure and the rejection rate of salt ions in feedwater by the membrane, respectively. For practical applications, it is imperative that these performance properties are not compromised by the membrane modification process.

The water permeability and salt rejection of the pristine TFC and modified membranes were measured in RO configuration using cross-flow cells under an applied hydraulic pressure of 24.1 bar (Figure 3). The water permeabilities of the membranes

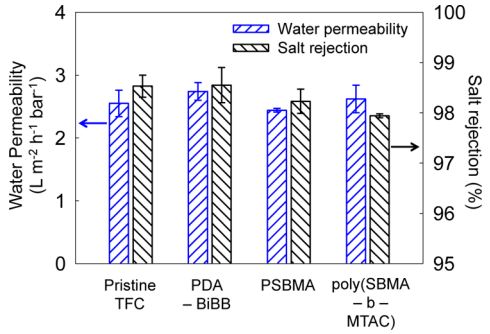

Figure 3. Membrane transport and performance properties of pristine, PDA-BiBB immobilized, PSBMA-grafted, and poly(SBMA-*b*-MTAC)-grafted TFC membranes, including the water permeability coefficient (L m^{-2} h^{-1} bar^{-1}) measured under an applied pressure of 24.1 bar (left) and salt (NaCl) rejection measured using an applied pressure of 24.1 bar and a feed solution of 50 mM NaCl (right).

consecutively modified with PDA-BiBB, PSBMA, and poly(SBMA-*b*-MTAC) are very similar to that of the pristine TFC membrane. These results are indicative of the minimal thicknesses of the deposited polymer layers.

To measure the salt rejection, we used a 50 mM NaCl feed solution under 24.1 bar applied pressure, and the salt concentration of the permeate was determined by measuring ionic conductivity. Salt rejections of the PDA-BiBB, PSBMA, and PMTAC membranes were only slightly reduced with the poly(SBMA-*b*-MTAC)-modified membrane exhibiting ~0.5% reduction in salt rejection (Figure 3). The salt permeability coefficient of the membrane, an intrinsic membrane property, was calculated from the measured salt rejection after accounting for the concentration polarization effect.[75] A small increase in the salt permeability coefficient is observed only for the final poly(SBMA-*b*-MTAC) (Figure S5). However, such a change in salt permeability does not compromise the applicability of the functionalized membrane for RO applications, as the functionalized membrane maintains good water permeability and salt rejection performance.

3.3. Protein Fouling Resistance and Antimicrobial Properties. *3.3.1. Adhesion Force Measurement.* Zwitterionic polymer coatings impart antifouling properties to surfaces by increasing the hydrophilicity of the surface.[17−21] To quantify how the addition of zwitterionic PSBMA brushes changed the fouling propensity of the membrane, we used chemical force microscopy to determine the adhesion forces between a colloidal probe attached to an AFM cantilever and the different functionalized membranes. The use of a carboxylated latex particle as a colloidal probe provides a general evaluation of foulant adhesion to the membrane[58] due to the involvement of carboxylic functional groups through calcium bridging in the adhesion of numerous types of organic foulants on membranes.[76−79] This approach allowed us to compare the fouling propensity of the modified TFC membrane and evaluate the contributions of the different components of the poly(SBMA-*b*-MTAC)-modified membrane to the fouling resistance of the final membrane.

For each step of the membrane modification with poly(SBMA-*b*-MTAC), the adhesion forces were quantified by more than 200 individual force measurements over five random locations on the membrane. The distributions of the maximum adhesion forces between the colloidal probe, serving as a general model for organic foulants, and the different membranes are shown in Figure 4. From the adhesion force distributions, important differences in the fouling propensity can be observed between the pristine TFC membrane and the modified membranes.

The pristine TFC membrane shows an average maximum adhesion force of −0.35 ± 0.30 mN/m with the majority of the force events being adhesive (negative values). We find that 27% of all measured events show no adhesion (NO column), indicating repulsive interactions of the foulant probe with the membrane (Figure 4a). The initial PDA-BiBB coating of the membrane increased the measured adhesion forces between the colloidal probe and the membrane, reaching an average adhesion force of −0.49 ± 0.30 mN/m (Figure 4b). However, upon grafting of PSBMA, the adhesion propensity of the colloidal probe was markedly decreased to −0.03 ± 0.30 mN/m with a majority (84%) of nonadhesion events (Figure 4c). This reduced fouling propensity of the PSBMA-modified membranes indicates a good coverage of the underlying PDA-BiBB by PSBMA, which swells in the presence of water. Swelling of polymer brushes can also contribute to reduction of the adhesion forces compared to the PDA-BiBB membrane by increasing the distance between the solid−water interface and the PDA-BiBB layer.

In comparison, a PMTAC-modified TFC membrane showed a fouling propensity between the pristine TFC membrane and the PSBMA membrane (Figure 4d). Although typically negatively charged foulants can be attracted to positively charged surfaces, the observed lower adhesion force on the PMTAC-modified membrane compared to the pristine TFC one may be attributed to enhanced hydrophilicity (Figure S2). This indicates that the antimicrobial QAS added to the membrane, although not as antifouling as PSBMA, should not significantly affect the antifouling capacity of the final poly(SBMA-*b*-MTAC). The adhesion forces measured for the poly(SBMA-*b*-MTAC) membrane are found to be in the same range as those of the PSBMA membrane (Figure 4e), also indicating that the addition of PMTAC did not have a

DOI: 10.1021/acsami.5b06647
ACS Appl. Mater. Interfaces 2015, 7, 23069−23079

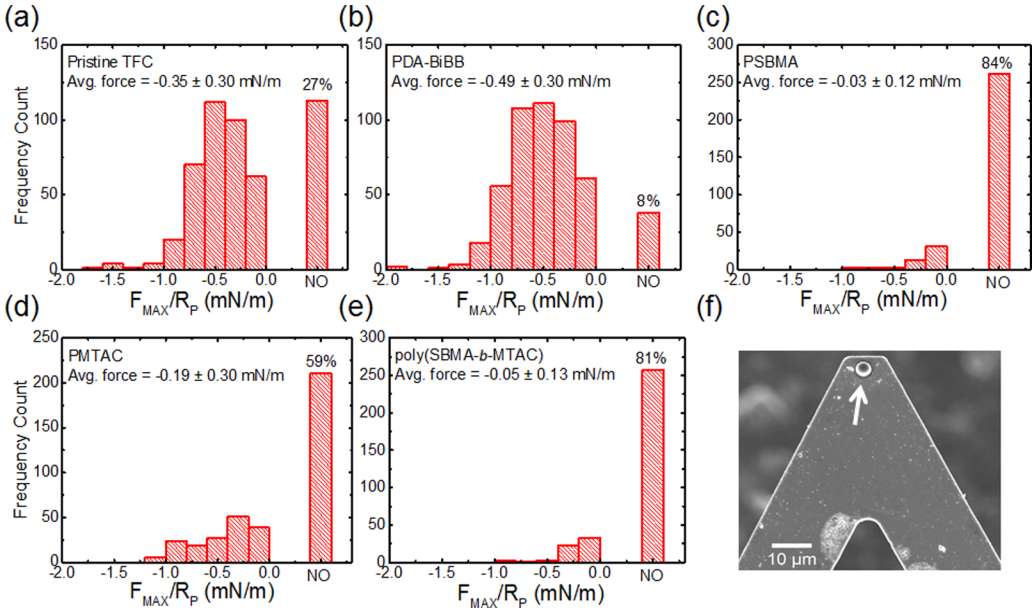

Figure 4. Adhesion force distributions between a carboxyl-modified latex particle probe and pristine (a), PDA-BiBB-immobilized (b), PSBMA-grafted (c), PMTAC-grafted (d), and poly(SBMA-*b*-MTAC)-grafted (e) TFC membranes. Forces are normalized by the diameter of the particle probe. The solution media used for AFM measurements contained 50 mM NaCl and 0.5 mM $CaCl_2$. The columns labeled "NO" indicate measurements where the probe−membrane interactions were too weak to be differentiated from random fluctuations and are considered as no adhesion. (f) Scanning electron microscopy micrograph of the functionalized cantilever used for adhesion force measurements with the arrow indicating the carboxylated latex particle.

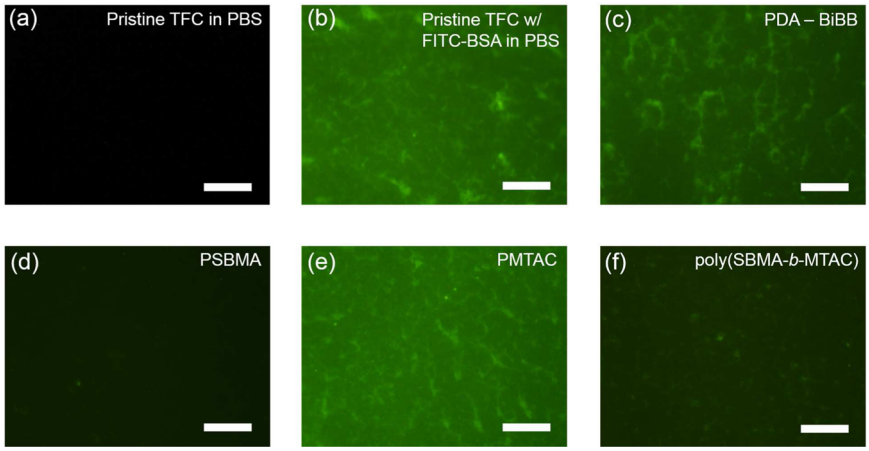

Figure 5. Epifluorescence microscope images of pristine and modified TFC membranes following protein adhesion tests using fluorescein-labeled BSA (BSA-FITC) in PBS. Pristine TFC membranes exposed to PBS without (a) and with BSA-FITC (b). PDA-BiBB-immobilized (c), PSBMA-grafted (d), PMTAC-grafted (e), and poly(SBMA-*b*-MTAC)-grafted (f) TFC membranes after exposure to PBS with BSA-FITC. The scale bar is 20 μm.

significant effect on the antifouling properties of the PSBMA layer.

3.3.2. BSA Adsorption Test. The antifouling character of the modified TFC membranes was confirmed using bovine serum albumin (BSA) as a model protein foulant. Proteins are ubiquitous foulants in typical feedwater sources. Proteins not only reduce water flux through membranes, but adsorbed proteins can also provide a conditioning layer for bacterial growth and biofilm formation, eventually leading to biofouling.[8] Therefore, prevention of attachment of proteins on membrane surfaces is critical for successful antifouling functionality.

As a model protein foulant, we used BSA that was fluorescein-tagged (FITC-BSA, A23015, Life Technologies). We allowed the pristine and modified membranes to be in contact with a solution of FITC-BSA (0.05 mg/mL) in PBS at pH 7.4 for 3 h in the dark. The fluorescence intensity of the FITC-BSA exposed membranes qualitatively shows the degree of adsorption of BSA on the membranes.

The FITC-BSA exposed pristine membrane emitted a high intensity of fluorescence (Figure 5b) compared to the membrane exposed to PBS alone (Figure 5a), indicating significant adsorption of BSA. Although BSA adsorption on the PDA-BiBB-modified membrane was somewhat reduced with slightly lower fluorescence intensity (Figure 5c), the PSBMA-modified membrane showed almost no adsorption of BSA without any noticeable fluorescence (Figure 5d). This observation clearly demonstrates that zwitterionic polymers are densely hydrated with water molecules, thereby preventing

DOI: 10.1021/acsami.5b06647
ACS Appl. Mater. Interfaces 2015, 7, 23069−23079

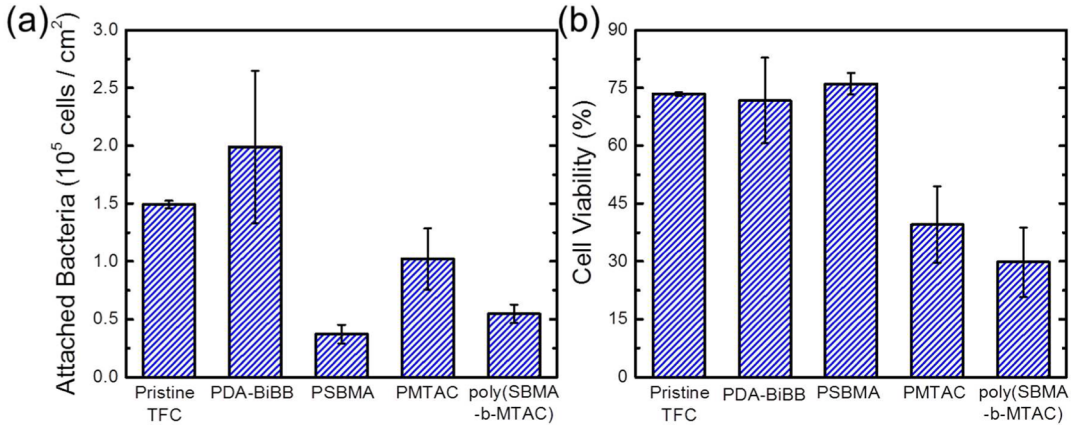

Figure 6. Adhesion and cell viability of *E. coli* cells on pristine and modified TFC membranes. (a) Total cell count of attached bacteria per membrane surface area. (b) Viability of *E. coli* cells attached to the membrane (contact time of 3 h at room temperature), as determined by the Syto 9/propidium iodide viability stain.

contact of BSA.[17−21] The membrane grafted with PMTAC only after PDA-BiBB (Figure 5e) shows almost the same fluorescence intensity as the pristine membrane, probably because BSA adsorption was promoted by electrostatic attraction between the positively charged QAS polymeric layer and the negatively charged BSA.[80] This seems to be a common disadvantage for membranes solely modified with bactericidal materials, which was also evidenced in previous studies.[42−44] Our final membrane modified with poly(SBMA-*b*-MTAC) (Figure 5e) exhibits slightly increased adsorption of BSA compared to that with PSBMA alone but is still significantly lower than that of the pristine membrane. This observation clearly indicates the antifouling property of our thin block copolymer-modified membrane.

3.3.3. Bacterial Adhesion and Inactivation. Bacterial adhesion and inactivation were also evaluated to determine the antibiofouling potential of the poly(SBMA-*b*-MTAC)-modified TFC membrane. Bacterial adhesion was measured after a 3 h exposure of the membrane surface to an *E. coli* suspension in PBS buffer (pH 7.4). The membranes were mildly washed to remove nonadhered cells and stained with Syto 9 and propidium iodide for cell enumeration and viability. Using this approach, both the total number of bacterial cells (adhesion) and the relative amount of live cells (cell viability) can be assessed.

Bacterial cell adhesion was found to follow the same trend as the fouling propensity measured by chemical force microscopy using the carboxylated latex colloidal probe. The number of bacterial cells adhered to the membrane surface after 3 h of contact decreased in the order PDA-BiBB > pristine > PMTAC > poly(SBMA-*b*-MTAC) > PSBMA (Figure 6a). Membranes with zwitterionic polymer coatings, i.e., PSBMA and poly(SBMA-*b*-MTAC), thus showed excellent resistance to bacterial adhesion, whereas membranes coated with PMTAC only showed a bacterial adhesion propensity halfway between pristine TFC membranes and PSBMA-grafted membranes. This observation is probably due to the electrostatic attraction between the negatively charged bacterial cell surfaces and the positive quaternary ammonium moieties as shown by zeta potential measurements (Figure 2b).

Only membranes with PMTAC QAS brushes were found to possess antimicrobial activity (Figure 6b), exhibiting a decrease from 73% of cell viability (pristine TFC) to 39 and 28% viability for PMTAC and poly(SBMA-*b*-MTAC)-modified TFC membranes, respectively. The addition of QAS induces disruption of the bacterial cell wall membrane due to cationic binding of positively charged QAS moieties to the cell wall,[81] thus imparting antimicrobial properties to the TFC membrane. PSBMA coating alone did not significantly affect the cell viability of adhered bacterial cells compared to the pristine TFC membrane (p = 0.40, determined by Student's t test). Therefore, despite the adhesion of bacterial cells to the poly(SBMA-*b*-MTAC) membrane being slightly higher (p = 0.057) then that to PSBMA alone, the coupling of antimicrobial QAS moieties to PSBMA can enhance the antibiofouling potential of TFC membranes.

The relationship between biofouling resistance and bacterial adhesion is of course not straightforward. Studies have shown that membrane coatings having lower protein and bacterial adhesion can still suffer from the formation of biofilms.[40,82] However, for the specific case of low fouling zwitterionic polymers, bacterial adhesion was found to be a reliable indicator of biofouling propensity.[40] The lower fouling propensity of the poly(SBMA-*b*-MTAC) TFC membrane, demonstrated using chemical force microscopy and both protein and bacterial adhesion, may therefore suggest the potential of this approach as a biofouling mitigation strategy. In addition, surface functionalization for antimicrobial surface activity was found to provide a higher biofouling resistance than that suggested by adhesion assays.[40] The dual functionality of the poly(SBMA-*b*-MTAC) membrane, which is both antifouling and antimicrobial, suggests the excellent potential of this type of functionalization for biofilm control in membrane processes.

4. CONCLUSION

We present a new, scalable macromolecular architecture for TFC membranes to integrate both "defending" and "attacking" strategies against biofouling. Antifouling zwitterionic polymer brushes and antimicrobial QAS polymer brushes were sequentially grown from the surface of TFC membranes via surface-initiated ARGET-ATRP, an industrially benign polymerization method. Mussel-inspired polydopamine chemistry was utilized for a convenient immobilization of initiator molecules (BiBB). The evolution of the structure, morphology, and hydrophilicity during the surface modification was confirmed by ATR FTIR spectra, zeta potential analysis, SEM, and water contact angle measurements. The diblock

DOI: 10.1021/acsami.5b06647
ACS Appl. Mater. Interfaces 2015, 7, 23069−23079

copolymer grafted TFC membrane maintained the water permeability and salt rejection of the native TFC membrane. Biofouling resistance and bacterial adhesion and inactivation were comprehensively evaluated using chemical force microscopy and protein/bacterial adhesion tests. Results demonstrated a low biofouling propensity and good antimicrobial activity for the modified TFC membrane. The developed dual functional TFC membrane has great potential for use in water purification and desalination by RO technology. Moreover, the integrated antibiofouling strategy through ARGET-ATRP architecture of a multifunctional block copolymer is applicable for surface modification of other water treatment membranes as well as materials for transportation, biomedical, and energy applications.

■ ASSOCIATED CONTENT

Supporting Information

The Supporting Information is available free of charge on the ACS Publications website at DOI: 10.1021/acsami.5b06647.

Thickness increase of PSBMA brushes on silicon wafer, SEM image of PMTAC layer, energy dispersive spectroscopy (EDS) analysis of PSBMA, analysis of surface roughness, and transport properties of the pristine TFC, PDA-BiBB, PSBMA, and poly(SBMA-*b*-MTAC)-modified membranes (PDF)

■ AUTHOR INFORMATION

Corresponding Authors

*E-mail: yegang@mail.tsinghua.edu.cn.
*E-mail: menachem.elimelech@yale.edu.

Notes

The authors declare no competing financial interest.

■ ACKNOWLEDGMENTS

G.Y. acknowledges support from the Program for Changjiang Scholars and Innovative Research Team in University (IRT13026) and the National Natural Science Foundation of China under Projects 51473087 and U1430234. J.L. acknowledges financial support from the Department of Defense through the Strategic Environmental Research and Development Program (SERDP, Project ER-2217). F.P. acknowledges financial support from the Natural Sciences and Engineering Research Council of Canada postdoctoral fellowship. Facilities used were supported by the Yale Institute of Nanoscale and Quantum Engineering (YINQE), Chemical and Biophysical Instrument Center (CBIC), and NSF MRSEC DMR 1119826.

■ REFERENCES

(1) Shannon, M. A.; Bohn, P. W.; Elimelech, M.; Georgiadis, J. G.; Marinas, B. J.; Mayes, A. M. Science and Technology for Water Purification in the Coming Decades. *Nature* **2008**, *452*, 301−310.

(2) Elimelech, M.; Phillip, W. A. The Future of Seawater Desalination: Energy, Technology, and the Environment. *Science* **2011**, *333*, 712−717.

(3) Bar-Zeev, E.; Passow, U.; Romero-Vargas Castrillón, S.; Elimelech, M. Transparent Exopolymer Particles: From Aquatic Environments and Engineered Systems to Membrane Biofouling. *Environ. Sci. Technol.* **2015**, *49*, 691−707.

(4) Habimana, O.; Semião, A. J. C.; Casey, E. The Role of Cell-Surface Interactions in Bacterial Initial Adhesion and Consequent Biofilm Formation on Nanofiltration/Reverse Osmosis Membranes. *J. Membr. Sci.* **2014**, *454*, 82−96.

(5) Al-Juboori, R. A.; Yusaf, T. Biofouling in Ro System: Mechanisms, Monitoring and Controlling. *Desalination* **2012**, *302*, 1−23.

(6) Rana, D.; Matsuura, T. Surface Modifications for Antifouling Membranes. *Chem. Rev.* **2010**, *110*, 2448−2471.

(7) Xu, G.; Wang, J.; Li, C. Strategies for Improving the Performance of the Polyamide Thin Film Composite (PA-TFC) Reverse Osmosis (RO) Membranes: Surface Modifications and Nanoparticles Incorporations. *Desalination* **2013**, *328*, 83−100.

(8) Banerjee, I.; Pangule, R. C.; Kane, R. S. Antifouling Coatings: Recent Developments in the Design of Surfaces that Prevent Fouling by Proteins, Bacteria, and Marine Organisms. *Adv. Mater.* **2011**, *23*, 690−718.

(9) Ni, L.; Meng, J.; Li, X.; Zhang, Y. Surface Coating On the Polyamide TFC RO Membrane for Chlorine Resistance and Antifouling Performance Improvement. *J. Membr. Sci.* **2014**, *451*, 205−215.

(10) Schlenoff, J. B. Zwitteration: Coating Surfaces with Zwitterionic Functionality to Reduce Nonspecific Adsorption. *Langmuir* **2014**, *30*, 9625−9636.

(11) Cho, Y.; Cho, D.; Park, J. H.; Frey, M. W.; Ober, C. K.; Joo, Y. L. Preparation and Characterization of Amphiphilic Triblock Terpolymer-Based Nanofibers as Antifouling Biomaterials. *Biomacromolecules* **2012**, *13*, 1606−1614.

(12) Li, X.; Cai, T.; Chung, T. Anti-Fouling Behavior of Hyperbranched Polyglycerol-Grafted Poly(ether sulfone) Hollow Fiber Membranes for Osmotic Power Generation. *Environ. Sci. Technol.* **2014**, *48*, 9898−9907.

(13) Yang, C.; Ding, X.; Ono, R. J.; Lee, H.; Hsu, L. Y.; Tong, Y. W.; Hedrick, J.; Yang, Y. Y. Brush-Like Polycarbonates Containing Dopamine, Cations, and Peg Providing a Broad-Spectrum, Antibacterial, and Antifouling Surface *via* One-Step Coating. *Adv. Mater.* **2014**, *26*, 7346−7351.

(14) Roosjen, A.; van der Mei, H. C.; Busscher, H. J.; Norde, W. Microbial Adhesion to Poly(Ethylene Oxide) Brushes: Influence of Polymer Chain Length and Temperature. *Langmuir* **2004**, *20*, 10949−10955.

(15) Cheng, G.; Xue, H.; Zhang, Z.; Chen, S.; Jiang, S. A Switchable Biocompatible Polymer Surface with Self-Sterilizing and Nonfouling Capabilities. *Angew. Chem., Int. Ed.* **2008**, *47*, 8831−8834.

(16) Kane, R. S.; Deschatelets, P.; Whitesides, G. M. Kosmotropes Form the Basis of Protein-Resistant Surfaces. *Langmuir* **2003**, *19*, 2388−2391.

(17) Laschewsky, A. Structures and Synthesis of Zwitterionic Polymers. *Polymers* **2014**, *6*, 1544−1601.

(18) Quintana, R.; Gosa, M.; Jańczewski, D.; Kutnyanszky, E.; Vancso, G. J. Enhanced Stability of Low Fouling Zwitterionic Polymer Brushes in Seawater with Diblock Architecture. *Langmuir* **2013**, *29*, 10859−10867.

(19) Zhang, Y.; Wang, Z.; Lin, W.; Sun, H.; Wu, L.; Chen, S. A Facile Method for Polyamide Membrane Modification by Poly(sulfobetaine methacrylate) to Improve Fouling Resistance. *J. Membr. Sci.* **2013**, *446*, 164−170.

(20) Huang, C.; Brault, N. D.; Li, Y.; Yu, Q.; Jiang, S. Controlled Hierarchical Architecture in Surface-Initiated Zwitterionic Polymer Brushes with Structurally Regulated Functionalities. *Adv. Mater.* **2012**, *24*, 1834−1837.

(21) Chen, S.; Zheng, J.; Li, L.; Jiang, S. Strong Resistance of Phosphorylcholine Self-Assembled Monolayers to Protein Adsorption: Insights Into Nonfouling Properties of Zwitterionic Materials. *J. Am. Chem. Soc.* **2005**, *127*, 14473−14478.

(22) Zhu, J.; Su, Y.; Zhao, X.; Li, Y.; Zhao, J.; Fan, X.; Jiang, Z. Improved Antifouling Properties of Poly(vinyl chloride) Ultrafiltration Membranes *via* Surface Zwitterionicalization. *Ind. Eng. Chem. Res.* **2014**, *53*, 14046−14055.

(23) Sun, Q.; Su, Y.; Ma, X.; Wang, Y.; Jiang, Z. Improved Antifouling Property of Zwitterionic Ultrafiltration Membrane Composed of Acrylonitrile and Sulfobetaine Copolymer. *J. Membr. Sci.* **2006**, *285*, 299−305.

DOI: 10.1021/acsami.5b06647
ACS Appl. Mater. Interfaces 2015, 7, 23069−23079

(24) Wang, T.; Wang, Y.; Su, Y.; Jiang, Z. Antifouling Ultrafiltration Membrane Composed of Polyethersulfone and Sulfobetaine Copolymer. *J. Membr. Sci.* **2006**, *280*, 343−350.
(25) Azari, S.; Zou, L. Fouling Resistant Zwitterionic Surface Modification of Reverse Osmosis Membranes Using Amino Acid L-Cysteine. *Desalination* **2013**, *324*, 79−86.
(26) Yang, R.; Xu, J.; Ozaydin-Ince, G.; Wong, S. Y.; Gleason, K. K. Surface-Tethered Zwitterionic Ultrathin Antifouling Coatings On Reverse Osmosis Membranes by Initiated Chemical Vapor Deposition. *Chem. Mater.* **2011**, *23*, 1263−1272.
(27) Yu, H.; Kang, Y.; Liu, Y.; Mi, B. Grafting Polyzwitterions Onto Polyamide by Click Chemistry and Nucleophilic Substitution On Nitrogen: A Novel Approach to Enhance Membrane Fouling Resistance. *J. Membr. Sci.* **2014**, *449*, 50−57.
(28) Azari, S.; Zou, L. Using Zwitterionic Amino Acid L-DOPA to Modify the Surface of Thin Film Composite Polyamide Reverse Osmosis Membranes to Increase their Fouling Resistance. *J. Membr. Sci.* **2012**, *401*−*402*, 68−75.
(29) Yang, R.; Jang, H.; Stocker, R.; Gleason, K. K. Synergistic Prevention of Biofouling in Seawater Desalination by Zwitterionic Surfaces and Low-Level Chlorination. *Adv. Mater.* **2014**, *26*, 1711−1718.
(30) Yang, R.; Gleason, K. K. Ultrathin Antifouling Coatings with Stable Surface Zwitterionic Functionality by Initiated Chemical Vapor Deposition (iCVD). *Langmuir* **2012**, *28*, 12266−12274.
(31) Rahaman, M. S.; Thérien-Aubin, H.; Ben-Sasson, M.; Ober, C. K.; Nielsen, M.; Elimelech, M. Control of Biofouling On Reverse Osmosis Polyamide Membranes Modified with Biocidal Nanoparticles and Antifouling Polymer Brushes. *J. Mater. Chem. B* **2014**, *2*, 1724.
(32) Banerjee, I.; Mondal, D.; Martin, J.; Kane, R. S. Photoactivated Antimicrobial Activity of Carbon Nanotube−Porphyrin Conjugates. *Langmuir* **2010**, *26*, 17369−17374.
(33) Liu, Y.; Leng, C.; Chisholm, B.; Stafslien, S.; Majumdar, P.; Chen, Z. Surface Structures of Pdms Incorporated with Quaternary Ammonium Salts Designed for Antibiofouling and Fouling Release Applications. *Langmuir* **2013**, *29*, 2897−2905.
(34) Blok, A. J.; Chhasatia, R.; Dilag, J.; Ellis, A. V. Surface Initiated Polydopamine Grafted Poly([2-(Methacryoyloxy)Ethyl]-Trimethylammonium Chloride) Coatings to Produce Reverse Osmosis Desalination Membranes with Anti-Biofouling Properties. *J. Membr. Sci.* **2014**, *468*, 216−223.
(35) Ni, L.; Meng, J.; Li, X.; Zhang, Y. Surface Coating On the Polyamide TFC RO Membrane for Chlorine Resistance and Antifouling Performance Improvement. *J. Membr. Sci.* **2014**, *451*, 205−215.
(36) Perreault, F.; Tousley, M. E.; Elimelech, M. Thin-Film Composite Polyamide Membranes Functionalized with Biocidal Graphene Oxide Nanosheets. *Environ. Sci. Technol. Lett.* **2014**, *1*, 71−76.
(37) Mollahosseini, A.; Rahimpour, A. Interfacially Polymerized Thin Film Nanofiltration Membranes on TiO_2 Coated Polysulfone Substrate. *J. Ind. Eng. Chem.* **2014**, *20*, 1261−1268.
(38) Vercellino, T.; Morse, A.; Tran, P.; Hamood, A.; Reid, T.; Song, L.; Moseley, T. The Use of Covalently Attached Organo-Selenium to Inhibit S. Aureus and E. Coli Biofilms on RO Membranes and Feed Spacers. *Desalination* **2013**, *317*, 142−151.
(39) Ben-Sasson, M.; Lu, X.; Bar-Zeev, E.; Zodrow, K. R.; Nejati, S.; Qi, G.; Giannelis, E. P.; Elimelech, M. In Situ Formation of Silver Nanoparticles on Thin-Film Composite Reverse Osmosis Membranes for Biofouling Mitigation. *Water Res.* **2014**, *62*, 260−270.
(40) Bernstein, R.; Freger, V.; Lee, J.; Kim, Y.; Lee, J.; Herzberg, M. 'Should I Stay Or Should I Go?' Bacterial Attachment *vs* Biofilm Formation on Surface-Modified Membranes. *Biofouling* **2014**, *30*, 367−376.
(41) Ostuni, E.; Chapman, R. G.; Liang, M. N.; Meluleni, G.; Pier, G.; Ingber, D. E.; Whitesides, G. M. Self-Assembled Monolayers that Resist the Adsorption of Proteins and the Adhesion of Bacterial and Mammalian Cells. *Langmuir* **2001**, *17*, 6336−6343.
(42) Mi, L.; Jiang, S. Integrated Antimicrobial and Nonfouling Zwitterionic Polymers. *Angew. Chem., Int. Ed.* **2014**, *53*, 1746−1754.
(43) Yu, Q.; Cho, J.; Shivapooja, P.; Ista, L. K.; López, G. P. Nanopatterned Smart Polymer Surfaces for Controlled Attachment, Killing, and Release of Bacteria. *ACS Appl. Mater. Interfaces* **2013**, *5*, 9295−9304.
(44) Yuan, S.; Wan, D.; Liang, B.; Pehkonen, S. O.; Ting, Y. P.; Neoh, K. G.; Kang, E. T. Lysozyme-Coupled Poly(Poly(ethylene glycol) methacrylate)−Stainless Steel Hybrids and their Antifouling and Antibacterial Surfaces. *Langmuir* **2011**, *27*, 2761−2774.
(45) Ho, C. H.; Tobis, J.; Sprich, C.; Thomann, R.; Tiller, J. C. Nanoseparated Polymeric Networks with Multiple Antimicrobial Properties. *Adv. Mater.* **2004**, *16*, 957−961.
(46) Zou, P.; Hartleb, W.; Lienkamp, K. It Takes Walls and Knights to Defend a Castle − Synthesis of Surface Coatings From Antimicrobial and Antibiofouling Polymers. *J. Mater. Chem.* **2012**, *22*, 19579.
(47) Cao, Z.; Mi, L.; Mendiola, J.; Ella-Menye, J.; Zhang, L.; Xue, H.; Jiang, S. Reversibly Switching the Function of a Surface Between Attacking and Defending Against Bacteria. *Angew. Chem., Int. Ed.* **2012**, *51*, 2602−2605.
(48) Ran, J.; Wu, L.; Zhang, Z.; Xu, T. Atom Transfer Radical Polymerization (ATRP): A Versatile and Forceful Tool for Functional Membranes. *Prog. Polym. Sci.* **2014**, *39*, 124−144.
(49) Barbey, R.; Lavanant, L.; Paripovic, D.; Schüwer, N.; Sugnaux, C.; Tugulu, S.; Klok, H. Polymer Brushes Via Surface-Initiated Controlled Radical Polymerization: Synthesis, Characterization, Properties, and Applications. *Chem. Rev.* **2009**, *109*, 5437−5527.
(50) Xia, J.; Matyjaszewski, K. Controlled/"Living" Radical Polymerization. Atom Transfer Radical Polymerization Catalyzed by Copper(I) and Picolylamine Complexes. *Macromolecules* **1999**, *32*, 2434−2437.
(51) Wang, J.; Matyjaszewski, K. Controlled/"Living" Radical Polymerization. Halogen Atom Transfer Radical Polymerization Promoted by a Cu(I)/Cu(11) Redox Process. *Macromolecules* **1995**, *28*, 7901−7910.
(52) Siegwart, D. J.; Oh, J. K.; Matyjaszewski, K. ATRP in the Design of Functional Materials for Biomedical Applications. *Prog. Polym. Sci.* **2012**, *37*, 18−37.
(53) Matyjaszewski, K. Atom Transfer Radical Polymerization (ATRP): Current Status and Future Perspectives. *Macromolecules* **2012**, *45*, 4015−4039.
(54) Matyjaszewski, K.; Dong, H.; Jakubowski, W.; Pietrasik, J.; Kusumo, A. Grafting from Surfaces for "Everyone": ARGET ATRP in the Presence of Air. *Langmuir* **2007**, *23*, 4528−4531.
(55) Jakubowski, W.; Min, K.; Matyjaszewski, K. Activators Regenerated by Electron Transfer for Atom Transfer Radical Polymerization of Styrene. *Macromolecules* **2006**, *39*, 39−45.
(56) Jakubowski, W.; Matyjaszewski, K. Activators Regenerated by Electron Transfer for Atom-Transfer Radical Polymerization of (Meth)Acrylates and Related Block Copolymers. *Angew. Chem., Int. Ed.* **2006**, *45*, 4482−4486.
(57) Zhu, B.; Edmondson, S. Polydopamine-Melanin Initiators for Surface-Initiated ATRP. *Polymer* **2011**, *52*, 2141−2149.
(58) Lee, S.; Elimelech, M. Relating Organic Fouling of Reverse Osmosis Membranes to Intermolecular Adhesion Forces. *Environ. Sci. Technol.* **2006**, *40*, 980−987.
(59) Mi, B.; Elimelech, M. Organic Fouling of Forward Osmosis Membranes: Fouling Reversibility and Cleaning without Chemical Reagents. *J. Membr. Sci.* **2010**, *348*, 337−345.
(60) Hutter, J. L.; Bechhoefer, J. Calibration of Atomic-Force Microscope Tips. *Rev. Sci. Instrum.* **1993**, *64*, 1868−1873.
(61) Lee, H.; Dellatore, S. M.; Miller, W. M.; Messersmith, P. B. Mussel-Inspired Surface Chemistry for Multifunctional Coatings. *Science* **2007**, *318*, 426−430.
(62) Cho, J. H.; Shanmuganathan, K.; Ellison, C. J. Bioinspired Catecholic Copolymers for Antifouling Surface Coatings. *ACS Appl. Mater. Interfaces* **2013**, *5*, 3794−3802.

DOI: 10.1021/acsami.5b06647
ACS Appl. Mater. Interfaces 2015, 7, 23069−23079

(63) Liu, X.; Deng, J.; Ma, L.; Cheng, C.; Nie, C.; He, C.; Zhao, C. Catechol Chemistry Inspired Approach to Construct Self-Cross-Linked Polymer Nanolayers as Versatile Biointerfaces. *Langmuir* **2014**, *30*, 14905−14915.
(64) Della Vecchia, N. F.; Luchini, A.; Napolitano, A.; D Errico, G.; Vitiello, G.; Szekely, N.; D Ischia, M.; Paduano, L. Tris Buffer Modulates Polydopamine Growth, Aggregation, and Paramagnetic Properties. *Langmuir* **2014**, *30*, 9811−9818.
(65) Sparnacci, K.; Antonioli, D.; Gianotti, V.; Laus, M.; Zuccheri, G.; Ferrarese Lupi, F.; Giammaria, T. J.; Seguini, G.; Ceresoli, M.; Perego, M. Thermal Stability of Functional P(S-r-MMA) Random Copolymers for Nanolithographic Applications. *ACS Appl. Mater. Interfaces* **2015**, *7*, 3920−3930.
(66) Keskin, D.; Clodt, J. I.; Hahn, J.; Abetz, V.; Filiz, V. Postmodification of PS-b-P4VP Diblock Copolymer Membranes by ARGET ATRP. *Langmuir* **2014**, *30*, 8907−8914.
(67) Zhong, P. S.; Widjojo, N.; Chung, T.; Weber, M.; Maletzko, C. Positively Charged Nanofiltration (NF) Membranes *via* UV Grafting on Sulfonated Polyphenylenesulfone (SPPSU) for Effective Removal of Textile Dyes from Wastewater. *J. Membr. Sci.* **2012**, *417*−*418*, 52−60.
(68) Kirby, B. J.; Hasselbrink, E. F. Zeta Potential of Microfluidic Substrates: 1. Theory, Experimental Techniques, and Effects on Separations. *Electrophoresis* **2004**, *25*, 187−202.
(69) Elimelech, M.; Chen, W. H.; Waypa, J. J. Measuring the Zeta (electrokinetic) Potential of Reverse Osmosis Membranes by a Streaming Potential Analyzer. *Desalination* **1994**, *95*, 269−286.
(70) Childress, A. E.; Elimelech, M. Effect of Solution Chemistry on the Surface Charge of Polymeric Reverse Osmosis and Nanofiltration Membranes. *J. Membr. Sci.* **1996**, *119*, 253−268.
(71) Elimelech, M.; O'Melia, C. R. Effect of Electrolyte Type on the Electrophoretic Mobility of Polystyrene Latex Colloids. *Colloids Surf.* **1990**, *44*, 165−178.
(72) Shi, Q.; Su, Y.; Zhao, W.; Li, C.; Hu, Y.; Jiang, Z.; Zhu, S. Zwitterionic Polyethersulfone Ultrafiltration Membrane with Superior Antifouling Property. *J. Membr. Sci.* **2008**, *319*, 271−278.
(73) Suhara, T.; Fukui, H.; Yamaguchi, M. Fine Silica Powder Modified with Quaternary Ammonium Groups 2. The Influence of Electrolyte and PH. *Colloids Surf., A* **1995**, *101*, 29−37.
(74) Ryou, M.; Lee, Y. M.; Park, J.; Choi, J. W. Mussel-Inspired Polydopamine-Treated Polyethylene Separators for High-Power Li-ion Batteries. *Adv. Mater.* **2011**, *23*, 3066−3070.
(75) Cath, T. Y.; Elimelech, M.; McCutcheon, J. R.; McGinnis, R. L.; Achilli, A.; Anastasio, D.; Brady, A. R.; Childress, A. E.; Farr, I. V.; Hancock, N. T.; Lampi, J.; Nghiem, L. D.; Xie, M.; Yip, N. Y. Standard Methodology for Evaluating Membrane Performance in Osmotically Driven Membrane Processes. *Desalination* **2013**, *312*, 31−38.
(76) Ang, W.; Elimelech, M. Protein (BSA) Fouling of Reverse Osmosis Membranes: Implications for Wastewater Reclamation. *J. Membr. Sci.* **2007**, *296*, 83−92.
(77) Tang, C. Y.; Leckie, J. O. Membrane Independent Limiting Flux for RO and NF Membranes Fouled by Humic Acid. *Environ. Sci. Technol.* **2007**, *41*, 4767−4773.
(78) Mo, Y.; Xiao, K.; Shen, Y.; Huang, X. A New Perspective on the Effect of Complexation between Calcium and Alginate On Fouling During Nanofiltration. *Sep. Purif. Technol.* **2011**, *82*, 121−127.
(79) Mo, Y.; Tiraferri, A.; Yip, N. Y.; Adout, A.; Huang, X.; Elimelech, M. Improved Antifouling Properties of Polyamide Nanofiltration Membranes by Reducing the Density of Surface Carboxyl Groups. *Environ. Sci. Technol.* **2012**, *46*, 13253−13261.
(80) Böhme, U.; Scheler, U. Effective Charge of Bovine Serum Albumin Determined by Electrophoresis Nmr. *Chem. Phys. Lett.* **2007**, *435*, 342−345.
(81) Kenawy, E.; Worley, S. D.; Broughton, R. The Chemistry and Applications of Antimicrobial Polymers: a State-of-the-Art Review. *Biomacromolecules* **2007**, *8*, 1359−1384.
(82) Miller, D. J.; Araújo, P. A.; Correia, P. B.; Ramsey, M. M.; Kruithof, J. C.; van Loosdrecht, M. C. M.; Freeman, B. D.; Paul, D. R.; Whiteley, M.; Vrouwenvelder, J. S. Short-Term Adhesion and Long-Term Biofouling Testing of Polydopamine and Poly(ethylene glycol) Surface Modifications of Membranes and Feed Spacers for Biofouling Control. *Water Res.* **2012**, *46*, 3737−3753.

DOI: 10.1021/acsami.5b06647
ACS Appl. Mater. Interfaces 2015, 7, 23069−23079